



CrossMark
click for updates

Cite this: *RSC Adv.*, 2014, 4, 44377

CO₂ atmosphere-enhanced methanol aromatization over the NiO-HZSM-5 catalyst

Junhui Li, Chao Hu, Kai Tong, Hao Xiang, Zhirong Zhu* and Zhonghua Hu

The aromatization of methanol over parent HZSM-5 and the modified NiO-HZSM-5 in a fixed-bed reactor was investigated under CO₂ and N₂ flow. The as-prepared catalysts were characterized by H₂-TPR, XRD, BET, NH₃-TPD, CO₂-TPD and probe-molecule reaction. Compared with parent HZSM-5 in CO₂ or N₂ flow and with NiO-HZSM-5 in N₂ flow, NiO-HZSM-5 showed greatly improved aromatization activity and BTX (benzene, toluene and xylene) yield in CO₂ atmosphere. This is attributed to the cooperation of acid sites with the activated CO₂ (over NiO species), which not only can effectively promote dehydrogenation of alkanes to form olefin intermediates, but also can accelerate dehydrogenation in the conversion of olefin intermediates to aromatics. In particular, an optimized NiO-HZSM-5 with 2.0 wt% NiO loading showed 50.1% total aromatic yield and 35.5% BTX yield in CO₂ atmosphere. It also showed high catalytic stability resulting from the restriction of coking due to its acidity, carbonaceous elimination by the activated CO₂-reacting deposited coke, and the suppressed reduction of highly active NiO species by activated CO₂.

Received 3rd July 2014
Accepted 4th September 2014

DOI: 10.1039/c4ra06572g

www.rsc.org/advances

1. Introduction

As a fundamental raw material, aromatic hydrocarbon is widely used in pharmaceuticals, pesticides, dyes and the polymer industry. Among the aromatic products, benzene, toluene and xylene (BTX) are especially considered to be strategic materials. Commercially, aromatic production is based on petrochemical processes. However, the declining oil supply makes it crucial to develop an alternative way to produce aromatics (especially BTX). Although methane aromatization, especially over Mo-containing zeolite catalysts, is a potential route for the synthesis of aromatics,¹⁻⁷ its low aromatic yield and high reaction temperature greatly limit its industrial application.

With the rapid development of the coal chemical industry, the conversion of methanol to aromatics (MTA) over zeolite has become a potential way of producing aromatics. The formation of olefins, olefin oligomerization, cyclization and subsequent dehydrogenation on acid sites are the key steps in this catalytic reaction.⁸⁻¹⁰ HZSM-5 zeolite is considered to be the appropriate catalytic material for this process, because of its adjustable acidic properties and regular, three-dimensional, 10-ring pore matching with BTX molecules.⁹ Modifying HZSM-5 with ZnO, NiO, Ag₂O, CuO, and Ga₂O₃ *etc.*,^{9,11-15} can improve aromatization activity owing to the interaction-dehydrogenation^{16,17} of metal oxides with acid sites. For example, Conte *et al.* obtained 55.1% aromatic yield over AgO/ZSM-5 catalyst.¹⁴ Zaidi *et al.*

reported a ZnO/CuO-HZSM-5 catalyst with 69% aromatic yield.¹⁸ In addition, modification with P₂O₅ or Mo₂C can increase the BTX selectivity of HZSM-5;^{19,20} hydrothermal treatment¹⁹ and mesopore structure^{10,21} can improve the aromatic diffusion. La species can improve the aromatic selectivity and stability of Zn-HZSM-5.²² However, both coke and hydrothermal dealumination deactivate Ag-HZSM-5,¹² and the hydrolysis of GaO bonds results in the deactivation of H-Ga-ZSM-5.²³ The addition of ZnO over CuO-HZSM-5 can reduce coke formation and retard deactivation.¹⁸ SnO₂/ZnO-modified HZSM-5 showed improved selectivity and yield of BTX compared with Zn/HZSM-5, while its catalytic stability was poor.²⁴ Recently, Song *et al.* reported that the introduction of *n*-butane to methanol decreased the rate of coke deposition and prolonged the lifetime of Zn-HZSM-5/HZSM-11 catalysts.²⁵ Zheng *et al.* claimed that the coupling conversion of methanol with 2,5-dimethylfuran over HZSM-5 exhibited improved BTX yield.²⁶

On the whole, although great progress has been achieved in methanol-to-aromatics production over modified HZSM-5, the high added-value product (BTX) yield is still low. Besides unsuitable acidity in the HZSM-5 channel and external acid sites going against BTX shape-selectivity,^{9,10,27} two other reasons for low BTX yield are that the alkane byproducts (especially propane and butane) formed on acid sites cannot be effectively converted to olefin intermediates,²⁴ and the hydrogen produced by dehydrogenation in the conversion of olefin intermediate to aromatics cannot be immediately eliminated *in situ*. The greenhouse gas CO₂ has been used as a weak oxidant in the dehydrogenation of alkanes to olefins²⁸⁻³⁰ and the aromatization of alkanes^{31,32} over NiO-loading catalysts; the CO₂ activated

Department of Chemistry, Tongji University, 1239, Siping Road, Shanghai 200092, China. E-mail: zhuzhirong@tongji.edu.cn; Fax: +86-21-65981097; Tel: +86-21-65982563

over the NiO species³³ can improve the activity of these reactions owing to its oxidative dehydrogenation and suppression of coke deposition.^{28,30} Thus, it is expected that the weak oxidizability of CO₂ could promote dehydrogenation of hydrocarbons in the MTA reaction over NiO-modified HZSM-5.

This paper investigates the influence of CO₂ atmosphere on the performance of MTA reaction over NiO-HZSM-5. The results showed that CO₂ activated over the NiO species can significantly promote methanol aromatization by means of its cooperation with acid sites, and it can suppress coke formation and the reduction of active NiO species. To the best of our knowledge, this work is the first one on the use of CO₂ atmosphere for methanol-to-aromatics reaction.

2. Experimental

2.1. Catalyst preparation

ZSM-5 zeolite, with a SiO₂/Al₂O₃ molar ratio of 45, was purchased from Fuxu Company of Shanghai. Firstly, it was converted to NH₄-type ZSM-5 by the conventional ion-exchange method with aqueous NH₄NO₃ solution. Then, it was dried in an oven at 303 K and subsequently calcined at 813 K for 1 h with a ramp of 3 K min⁻¹ to obtain H-type ZSM-5. The HZSM-5 was pressed, crushed, and sorted to get parent HZSM-5 catalysts (particles of 12–20 mesh, denoted as Parent-Z). NiO-HZSM-5 was prepared by impregnation of parent HZSM-5 with Ni(NO₃)₂·6H₂O aqueous solution and calcination at 823 K for 1 h after drying. The modified catalyst was denoted as NiO-Z.

2.2. Catalyst characterization

The crystal structure of the catalysts was studied by X-ray diffraction analysis (XRD, D8ADVANCE) using Cu K α radiation. The specific surface area and pore volume were measured by N₂ adsorption–desorption at 77 K (NOVA 2200e, Quantachrome). NH₃-TPD and CO₂-TPD experiments were performed on a conventional set-up equipped with a TCD (CHEMBET 3000). The samples (200 mg) were first treated at 773 K in N₂ for 1 h, cooled to the adsorption temperature (393 K for NH₃-TPD, 373 K for CO₂-TPD), and then exposed to 45 ml min⁻¹ adsorption gas (20% NH₃ or 20% CO₂, N₂ in balance) for 60 min. The samples then were purged with N₂ at the adsorption temperature for 1 h and heated linearly at 10 K min⁻¹ to 873 K (NH₃-TPD) or 773 K (CO₂-TPD) in 45 ml min⁻¹ N₂. NH₃ or CO₂ in effluent was recorded continuously as a function of temperature. H₂-TPR of catalysts was also performed on a conventional set-up equipped with a TCD (CHEMBET 3000). Samples (200 mg) were first treated at 773 K in N₂ for 1 h, then cooled to 373 K. They were then shifted to 10% H₂-N₂ and heated linearly at 10 K min⁻¹ to 1073 K. The constraint index (CI) was determined with a fixed-bed micro-reactor and 1/1 hexane/3-methylpentane as the mixed reactants, 1.0 h⁻¹ WHSV under 10–60% total conversion, in helium flow at atmosphere pressure. The products were analyzed using on-line gas chromatography (HP5890) with a 50 m HP-PLOT/Al₂O₃ “S” capillary column and FID, and the constraint index (CI) was calculated according to the reported method.³⁴ The coke on the used catalysts was analysed by

thermogravimetric analysis (Netzsch STA 449C, Germany). Removing coke from the used catalysts (3.0 g) was achieved through calcining (in a tubular furnace with a 20 ml min⁻¹ air flow) at 813 K for 2 h with a ramp of 3 K min⁻¹.

2.3. Catalytic reaction

The prepared catalyst (5.0 g) was packed into a stainless steel, tubular fixed-bed reactor with 1.5 cm inner diameter and pre-treated in high-purity nitrogen flow at 823 K for 1 h. After decreasing the temperature to 783 K, methanol was pumped into the reactor by a metering pump. Aromatization was carried out at 1.0 h⁻¹ WHSV in 40 ml min⁻¹ CO₂ or N₂ flow. The effluent liquid was analyzed by an HP-5890 gas chromatograph equipped with a FID detector and a 50 m HP-FFAP capillary column. C₁–C₆₊ aliphatics in tail gas were analyzed by a HP-5890 gas chromatograph equipped with a FID detector and a 50 m HP-PLOT/Al₂O₃ “S” capillary column. CO, CO₂ and H₂ in tail gas were analyzed by a Shimadzu GC-8A gas chromatograph equipped with a TCD detector and a 10 m TDX01 molecular sieve column. The probe reaction, propane aromatization, was carried out at 783 K, 200 h⁻¹ GHSV (propane) and atmospheric pressure in the fixed-bed reactor with a mixed-gas flow (C₃H₈/N₂ (or CO₂) = 1.0 (ml/ml)). The product analysis was the same as that for methanol aromatization.

3. Results and discussion

3.1. Physicochemical properties of the prepared catalysts

The H₂-TPR results of modified HZSM-5 are shown in Fig. 1. As can be seen, the nickel oxide mainly existed as NiO on the surface of these catalysts. The major peak at about 855 K was assigned to the reduction of the “free state” NiO,³⁵ and the peak at about 1000 K was ascribed to the reduction of the “bound state” NiO species, which has the strong interaction with HZSM-5.^{36,37} With the increase of NiO content, the major peak shifted to a lower temperature due to the slight decrease of NiO dispersion.³⁸ The gradual evolution of a high-temperature peak implies that much “bound state” NiO appears on the catalysts with large loading.

Fig. 2 shows the XRD patterns of the prepared catalysts. NiO-HZSM-5 showed similar peaks to the parent HZSM-5, and no new diffraction peak appeared after modification. This suggests that the structure of HZSM-5 was not changed, and no new phase was produced during NiO modification.

As shown in Table 1, the regular decrease of micropore surface area, micropore volume, external surface and mesoporous volume for NiO-modified HZSM-5 suggests that NiO was not only loaded on the external surface of HZSM-5, but also into the channels.³⁹

In general, loading an adequate amount of metal oxide on HZSM-5 can narrow the pore diameter or pore opening and can enhance its molecular shape-selectivity in catalytic reaction.^{40,41} The change in pore size was usually determined by the constraint index (CI) based on the cracking reaction of probe molecules.^{27,42} As shown in Table 2, the CI values of parent HZSM-5 and NiO-modified HZSM-5 were almost equal,

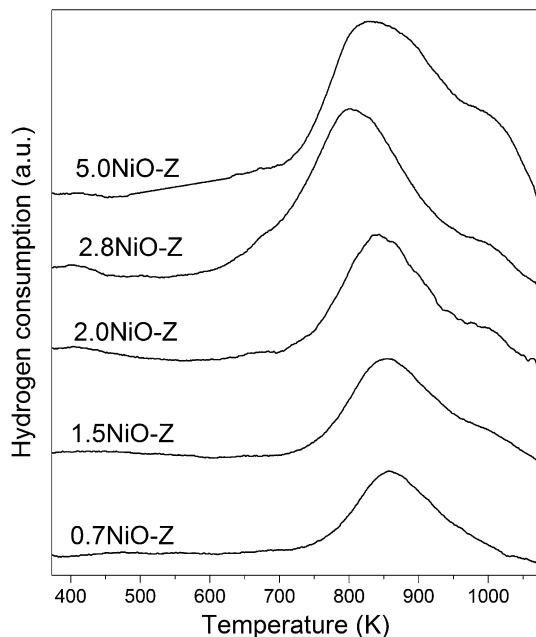


Fig. 1 H₂-TPR results of nickel oxide-modified HZSM-5.

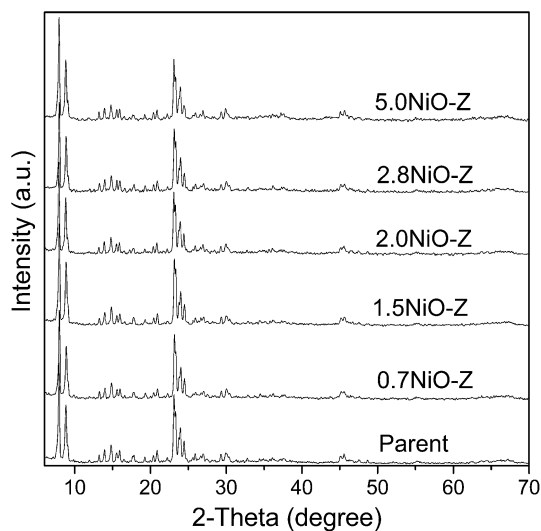


Fig. 2 XRD patterns of parent HZSM-5 and NiO-modified HZSM-5.

Table 1 Specific surface areas and pore volumes of parent HZSM-5 and NiO-modified HZSM-5

| Catalyst | Surface area (m ² g ⁻¹) | | | Pore volume (ml g ⁻¹) | |
|----------|--|----------|----------|-----------------------------------|-----------|
| | Total (BET) | External | Internal | Mesopore | Micropore |
| Parent-Z | 338.3 | 58.8 | 279.5 | 0.061 | 0.120 |
| 0.7NiO-Z | 334.1 | 56.4 | 277.7 | 0.059 | 0.119 |
| 1.5NiO-Z | 329.5 | 53.9 | 275.6 | 0.058 | 0.117 |
| 2.0NiO-Z | 325.4 | 52.1 | 273.3 | 0.056 | 0.115 |
| 2.8NiO-Z | 319.7 | 49.8 | 269.9 | 0.054 | 0.112 |
| 5.0NiO-Z | 302.6 | 42.5 | 260.1 | 0.049 | 0.105 |

Table 2 The constraint index (CI) of the parent HZSM-5 and NiO-modified HZSM-5

| Catalyst | Parent-Z | 0.7NiO-Z | 1.5NiO-Z | 2.0NiO-Z | 2.8NiO-Z | 5.0NiO-Z |
|----------|----------|----------|----------|----------|----------|----------|
| CI value | 6.05 | 6.05 | 6.06 | 6.06 | 6.07 | 6.08 |

implying that NiO ($\leq 5.0\%$) modification hardly enhanced the shape-selectivity of the HZSM-5 channel.

Fig. 3 shows the NH₃-TPD results of the prepared catalysts. The peaks below 573 K were assigned to the desorption of NH₃ adsorbed on weak acid sites, and the peaks above 573 K corresponded to strong acid sites.^{43,44} The desorption peaks (especially high-temperature peaks) shifted to a lower temperature, and their intensity weakened after modification. This suggests that NiO species covered the partial acid sites of HZSM-5 during modification and resulted in the lower acidic density of modified HZSM-5.⁴⁵ Moreover, strong acid sites were preferentially neutralized. As a result, 5.0NiO-Z showed the lowest acidic density and acidic strength, owing to its highest loading.

Fig. 4 shows the CO₂-TPD results of the prepared catalysts. The two peaks at about 435 K and 485 K were ascribed to the desorption of weakly adsorbed CO₂, and another peak at about 640 K corresponded to strongly adsorbed CO₂.^{46,47} The low-temperature desorption peaks shifted to a higher temperature after NiO modification. Moreover, the intensity of the high-temperature desorption peak increased with the increase of NiO loading, although it decreased beyond 2.0 wt%. The above changes indicate that the appropriate amount of NiO loading can obviously enhance the CO₂ adsorptivity of HZSM-5 thanks to the basic NiO species, which serves as adsorbing sites for CO₂.

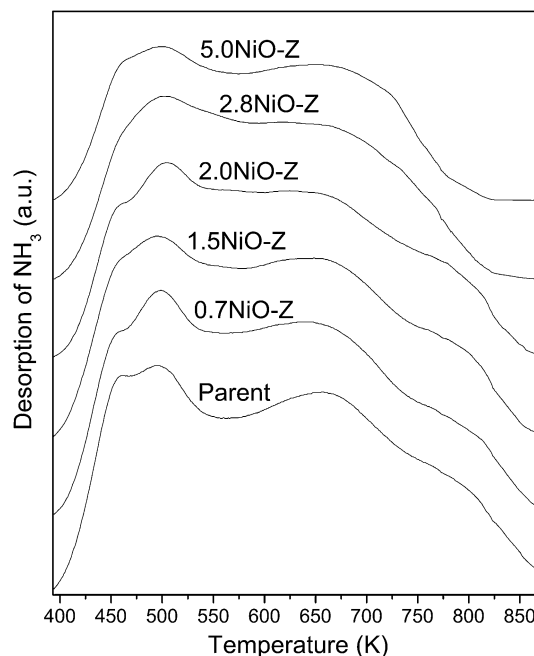


Fig. 3 NH₃-TPD results of parent HZSM-5 and NiO-modified HZSM-5.

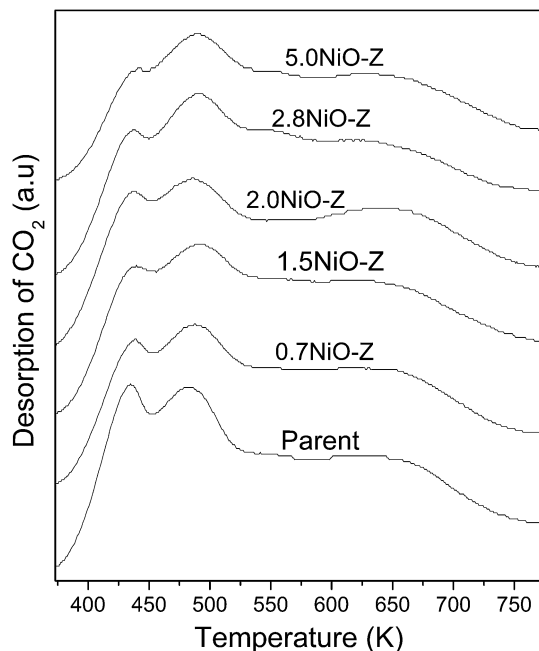


Fig. 4 CO₂-TPD results of parent HZSM-5 and NiO-modified HZSM-5.

molecules.³³ As a result, 2.0NiO-Z showed the strongest adsorptivity. Besides, the adsorptivity of 2.8NiO-Z and 5.0NiO-Z were slightly weaker than that of 2.0NiO-Z; this may result from their relatively small pore volumes and low NiO dispersion.

3.2. Methanol aromatization over the prepared catalysts in N₂ and CO₂ atmospheres

The yields of total aromatics and BTX in the MTA reaction over the prepared catalysts in N₂ and CO₂ atmospheres are shown in Table 3. As can be seen, total aromatic yield and BTX yield increased with NiO amounts below 2.0 wt%, especially in CO₂ atmosphere. However, excessive loading was detrimental to aromatization owing to the great weakening of acidity for 2.8NiO-Z and 5.0NiO-Z. 50.1% total aromatic yield and 35.5% BTX yield were obtained over 2.0NiO-Z catalyst in CO₂ atmosphere.

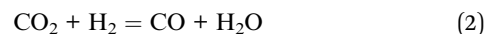
Table 3 The total aromatics yield, BTX selectivity and BTX yield over the prepared catalysts in N₂ and CO₂ atmospheres^a

| Catalysts | Total aromatic yield (%) | | BTX selectivity in aromatics (%) | | BTX yield (%) | |
|-----------|--------------------------|-----------------|----------------------------------|-----------------|----------------|-----------------|
| | N ₂ | CO ₂ | N ₂ | CO ₂ | N ₂ | CO ₂ |
| Parent-Z | 32.0 | 32.2 | 56.6 | 57.1 | 18.1 | 18.4 |
| 0.7NiO-Z | 32.8 | 36.6 | 60.1 | 68.3 | 19.7 | 25.0 |
| 1.5NiO-Z | 34.1 | 42.1 | 58.7 | 67.0 | 20.0 | 28.2 |
| 2.0NiO-Z | 35.0 | 50.1 | 67.4 | 70.9 | 23.6 | 35.5 |
| 2.8NiO-Z | 33.1 | 44.2 | 71.3 | 65.6 | 23.6 | 29.0 |
| 5.0NiO-Z | 30.5 | 39.7 | 69.2 | 65.7 | 21.1 | 26.1 |

^a MTA reaction was carried out at 783 K and 1.0 h⁻¹ WHSV in a 40 ml min⁻¹ CO₂ or N₂ flow. Product samples were tested at 1.0 h.

Comparatively, those were only about 32% and 18% over parent-Z, respectively. Moreover, although the interaction¹⁴ of NiO with acid sites slightly improved aromatization over NiO-Z in N₂ atmosphere, the product yield was still relatively low. These results strongly suggest that the integration of CO₂ atmosphere and NiO loading significantly enhanced the aromatization activity and BTX yield in the MTA reaction over HZSM-5.

Ding *et al.* pointed out that NiO species is highly active for the coupled dehydrogenation of isobutane with CO₂ over NiO_x/AC (nickel supported on active carbon) catalyst.³⁰ This coupled reaction is described as follows:



The reverse water-gas shift reaction of CO₂ (activated by NiO species) with the hydrogen from isobutane dehydrogenation enhanced the isobutene yield to form CO. A similar result was also obtained over NiO/Al₂O₃ catalyst.²⁸ Owing to the dehydrogenation of hydrocarbon in aromatization, H₂ can be produced in the MTA reaction. As listed in Table 4, the H₂ yield (below 0.16%) over NiO-Z in CO₂ atmosphere was much lower than those (above 1.0%) on parent-Z in the two atmospheres and over NiO-Z under N₂ atmosphere, while the CO yield was much higher (above 2.10%). This proves that the dehydrogenation of hydrocarbon in the aromatization over NiO-HZSM-5 under CO₂ atmosphere was coupled with the reverse water-gas shift reaction by CO₂ activated over the NiO species. Besides, the small amount of CO (below 0.28%) over parent-Z under the two atmospheres and over NiO-Z under N₂ atmosphere was produced by the decomposition of methanol without acidic adsorption,⁴⁸ and the water-gas reaction⁴⁹ of the deposited carbon with the water formed by methanol dehydration.

The distribution of xylene isomers was at the thermodynamic equilibrium value in the MTA reaction over all the prepared catalysts, and the total aromatic yield was similar over these catalysts in N₂ atmosphere. This again proves that NiO modification had no enhancement on the shape selectivity of HZSM-5 channel and indicates that the changes in product distribution for modified HZSM-5 are unrelated to porous shape-selectivity. Because the pore diameter of HZSM-5 is near the molecular size of xylene,⁹ enhanced shape-selectivity of the channel can restrict formation or diffusion of alkylbenzenes with relatively large molecular size, resulting in the increase of *para*-selectivity of xylene^{27,39-41} and decrease of total aromatic selectivity.²⁷ Significantly, hydrocarbon yield was similar for the prepared catalysts in the two atmospheres. The selectivity of total aliphatics, total alkanes and total olefins over NiO-Z in CO₂ atmosphere was much lower than that under N₂ atmosphere, while total aromatic selectivity was much higher. Olefins are the intermediates of aromatization. Increasing olefin intermediates *in situ*²⁴ and accelerating the dehydrogenation in the subsequent conversion of olefin intermediates to aromatics³⁰ are two effective ways to enhance the aromatic yield. Moreover, the conversion of olefin to aromatics occurs more easily than dehydrogenation of alkanes in this reaction.²⁴ Thus, it can be

Table 4 The detailed results of MTA reaction over parent HZSM-5 and NiO-HZSM-5 in N₂ and CO₂ atmospheres^a

| Catalyst/atmosphere | Parent-Z/N ₂ | Parent-Z/CO ₂ | 1.5NiO-Z/N ₂ | 1.5NiO-Z/CO ₂ | 2.0NiO-Z/N ₂ | 2.0NiO-Z/CO ₂ | 5.0NiO-Z/N ₂ | 5.0NiO-Z/CO ₂ |
|---|-------------------------|--------------------------|-------------------------|--------------------------|-------------------------|--------------------------|-------------------------|--------------------------|
| Hydrocarbon yield (%) | 97.8 | 97.5 | 98.6 | 97.6 | 98.2 | 97.0 | 98.0 | 97.2 |
| Hydrocarbon distribution (%) | | | | | | | | |
| CH ₄ | 3.79 | 5.11 | 4.48 | 3.41 | 4.18 | 7.05 | 5.92 | 5.03 |
| C ₂ H ₆ | 1.63 | 2.13 | 3.12 | 3.81 | 4.51 | 5.01 | 2.98 | 3.81 |
| C ₂ H ₄ | 1.62 | 1.24 | 3.14 | 2.04 | 2.34 | 1.55 | 3.02 | 2.34 |
| C ₃ H ₈ | 25.72 | 28.41 | 17.36 | 18.36 | 18.06 | 12.54 | 17.02 | 15.86 |
| C ₃ H ₆ | 2.49 | 2.29 | 6.15 | 3.68 | 4.28 | 2.93 | 6.02 | 4.95 |
| <i>i</i> -C ₄ H ₁₀ | 15.74 | 13.86 | 14.22 | 12.50 | 13.37 | 8.92 | 13.68 | 11.63 |
| <i>n</i> -C ₄ H ₁₀ | 6.49 | 6.14 | 5.08 | 4.68 | 4.97 | 3.26 | 4.93 | 4.37 |
| <i>t</i> -2-C ₄ H ₈ | 0.41 | 0.39 | 0.91 | 0.51 | 0.71 | 0.46 | 1.02 | 0.55 |
| 1-C ₄ H ₈ | 0.29 | 0.22 | 0.59 | 0.23 | 0.46 | 0.27 | 0.60 | 0.29 |
| <i>i</i> -C ₄ H ₈ | 0.83 | 0.77 | 2.01 | 0.87 | 1.33 | 0.92 | 2.05 | 1.26 |
| <i>c</i> -2-C ₄ H ₈ | 0.29 | 0.25 | 0.69 | 0.29 | 0.50 | 0.32 | 0.80 | 0.48 |
| C ₅ | 7.21 | 5.76 | 7.17 | 6.04 | 8.95 | 4.85 | 9.97 | 8.21 |
| C ₆₊ | 0.80 | 0.43 | 0.49 | 0.50 | 0.73 | 0.22 | 0.91 | 0.43 |
| B | 1.81 | 1.25 | 1.01 | 2.53 | 1.98 | 3.84 | 1.79 | 2.01 |
| T | 4.73 | 5.53 | 6.44 | 10.49 | 7.64 | 12.47 | 6.80 | 8.54 |
| EB | 0.50 | 0.43 | 0.62 | 0.63 | 0.59 | 0.87 | 0.58 | 0.66 |
| <i>p</i> -X | 2.80 | 2.89 | 3.15 | 3.97 | 3.47 | 4.89 | 3.14 | 3.92 |
| <i>m</i> -X | 6.29 | 6.36 | 6.71 | 8.26 | 7.57 | 10.69 | 6.78 | 8.56 |
| <i>o</i> -X | 2.88 | 2.84 | 2.97 | 3.64 | 3.37 | 4.71 | 3.02 | 3.82 |
| C ₉ | 7.80 | 7.62 | 6.64 | 7.52 | 5.79 | 7.71 | 5.58 | 8.09 |
| C ₁₀ | 4.15 | 4.87 | 5.97 | 5.03 | 4.30 | 5.38 | 2.79 | 4.2 |
| Other aromatics | 1.73 | 1.21 | 1.08 | 1.01 | 0.90 | 1.14 | 0.60 | 0.99 |
| Total aliphatics | 67.31 | 67.00 | 65.41 | 56.92 | 64.39 | 48.30 | 68.92 | 59.21 |
| Total alkanes | 60.58 | 61.32 | 50.13 | 48.31 | 53.07 | 41.09 | 52.88 | 47.65 |
| Total olefins | 6.73 | 5.68 | 15.28 | 8.61 | 11.32 | 7.21 | 16.04 | 11.56 |
| Total aromatics | 32.69 | 33.00 | 34.59 | 43.08 | 35.61 | 51.70 | 31.08 | 40.79 |
| BTX | 18.51 | 18.87 | 20.28 | 28.89 | 24.03 | 36.6 | 21.53 | 26.85 |
| Non-hydrocarbon yield (%) | | | | | | | | |
| H ₂ | 1.11 | 1.03 | 1.01 | 0.15 | 1.26 | 0.06 | 1.41 | 0.05 |
| CO | 0.15 | 0.14 | 0.18 | 2.10 | 0.20 | 2.80 | 0.27 | 2.61 |
| CO ₂ | 0.09 | | 0.11 | | 0.15 | | 0.16 | |

^a C₅: C₅ aliphatics; C₆₊: C₆₊ aliphatics; B: benzene; T: toluene; EB: ethylbenzene; *p*-X: *para*-xylene; *m*-X: *meta*-xylene; *o*-X: *ortho*-xylene; C₉: C₉ aromatics; C₁₀: C₁₀ aromatics. MTA reaction was carried out at 783 K and 1.0 h⁻¹ WHSV in a 40 ml min⁻¹ CO₂ or N₂ flow. Product samples were tested at 1.0 h; conversion of methanol was 100% over these prepared catalysts.

confirmed that the coupled reaction not only can effectively promote dehydrogenation of alkanes to form olefin intermediates, but also can accelerate dehydrogenation in the conversion of olefin intermediates to aromatics over NiO-HZSM-5 in CO₂ atmosphere. Of course, the diffusion of hydrocarbon species is very important. On the one hand, the alkanes formed from methanol and the intermediates (for example, formed by cyclization of olefins) in the conversion of olefins to aromatics on acid sites must be desorbed and diffuse to react with CO₂ activated over the NiO species. On the other hand, the species formed by their dehydrogenation through reacting with activated CO₂ must diffuse to be adsorbed on acid sites for the subsequent reaction. Under the cooperation of acid sites with the CO₂ activated over NiO species, the conversion of aliphatics to aromatics was promoted, and aromatization activity was enhanced in the MTA reaction. In addition, as listed in Tables 3 and 4, NiO-Z in CO₂ atmosphere showed much higher BTX selectivity than parent-Z. This is due to the promoting effect of

the coupled reaction on the conversion of aliphatics to BTX and the weaker acidity of NiO-Z, which can suppress the deep reaction of BTX.⁵¹ Owing to its strongest CO₂ adsorptivity, the highest total aromatic yield and BTX yield were obtained over 2.0NiO-Z with appropriate acidity.

The main alkane product was propane over the prepared catalysts in MTA reaction. Therefore, as the probe reaction, propane aromatization was investigated over parent-Z and 2.0NiO-Z in the two atmospheres to evaluate the effect of CO₂ atmosphere. The detailed results are listed in Table 5. As can be seen, reaction results were very similar over parent-Z in N₂ and CO₂ atmospheres. Although 2.0NiO-Z showed weaker acidity than parent-Z, it exhibited slightly higher propane conversion (41.54%) and aromatic selectivity (31.76%) in N₂ atmosphere, owing to the interaction-dehydrogenation of NiO species with acid sites.¹⁴ Significantly, much higher propane conversion (62.73%) and aromatic selectivity (49.44%) were obtained on 2.0NiO-Z in CO₂ atmosphere. There are two ways of propane

Table 5 The results of propane aromatization over parent HZSM-5 and 2.0% NiO-HZSM-5 in N₂ and CO₂ atmospheres^a

| Catalysts | Parent-Z/N ₂ | Parent-Z/CO ₂ | 2.0NiO-Z/N ₂ | 2.0NiO-Z/CO ₂ |
|---------------------------------|-------------------------|--------------------------|-------------------------|--------------------------|
| Propane conversion (%) | 35.71 | 36.30 | 41.54 | 62.73 |
| Product distribution (%) | | | | |
| CH ₄ | 16.32 | 17.50 | 14.77 | 8.64 |
| C ₂ H ₄ | 14.82 | 13.62 | 13.88 | 9.80 |
| C ₂ H ₆ | 12.26 | 12.68 | 11.76 | 8.58 |
| C ₃ H ₆ | 11.88 | 12.15 | 12.23 | 9.09 |
| C ₄₊ aliphatics | 14.24 | 14.13 | 15.60 | 14.45 |
| Benzene | 9.17 | 8.86 | 9.86 | 13.92 |
| Toluene | 13.34 | 13.15 | 14.23 | 22.83 |
| Xylene | 7.45 | 7.22 | 6.97 | 11.43 |
| EB + C ₉ | 0.52 | 0.69 | 0.70 | 1.26 |
| Aromatic selectivity (%) | 30.48 | 29.92 | 31.76 | 49.44 |
| H ₂ yield (%) | 1.67 | 1.71 | 1.90 | 0.14 |
| CO yield (%) | 0.10 | 0.12 | 0.15 | 2.85 |

^a EB: ethylbenzene; C₉: C₉ aromatics; propane aromatization was carried out at 783 K, 200 h⁻¹ GHSV (propane) and atmospheric pressure on the fixed-bed reactor with a mixed gas flow (C₃H₈/N₂ (or CO₂) = 1.0 (ml ml⁻¹)); product samples were tested at 1.0 h.

decomposition on acid sites in this reaction: decomposing to form propylene through the hydrogen abstraction reaction of carbonium ion, and cracking to form ethylene and methane.⁵² Aromatics are formed from olefins.⁵⁰ As listed in Table 5, the H₂ yield (0.14%) over 2.0NiO-Z in CO₂ atmosphere was much lower than those (above 1.66%) on parent-Z in the two atmospheres and over NiO-Z under N₂ atmosphere, but CO yield was much higher. Moreover, although the highest propane conversion was obtained over 2.0NiO-Z in CO₂ atmosphere, methane and olefin selectivity were lowest. These imply that the CO₂ activated over NiO species not only can promote the dehydrogenation of propane to produce more propylene intermediate, but also can accelerate the dehydrogenation of the intermediates in the conversion of olefins to aromatics, enhancing aromatic yield by means of its cooperation with acid sites on this catalyst. Furthermore, this result powerfully proves the promoting effect of the coupled reaction on methanol aromatization over NiO-HZSM-5 under CO₂ atmosphere. To clearly explain this process, a conceptual diagram is shown in Fig. 5.

3.3. Catalytic stability of 2.0% NiO-HZSM-5 in the MTA reaction under CO₂ atmosphere

Fig. 6 shows the comparison of the catalytic stability of parent-Z and 2.0NiO-Z under N₂ and CO₂ atmospheres. As can be seen,

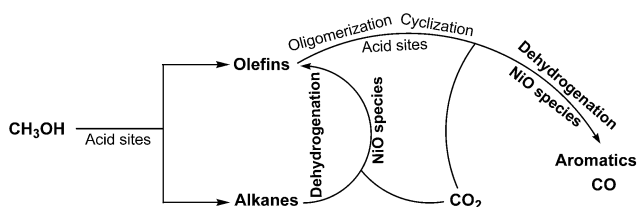


Fig. 5 Schematic of the promoting effect of CO₂ atmosphere on methanol aromatization over NiO-HZSM-5.

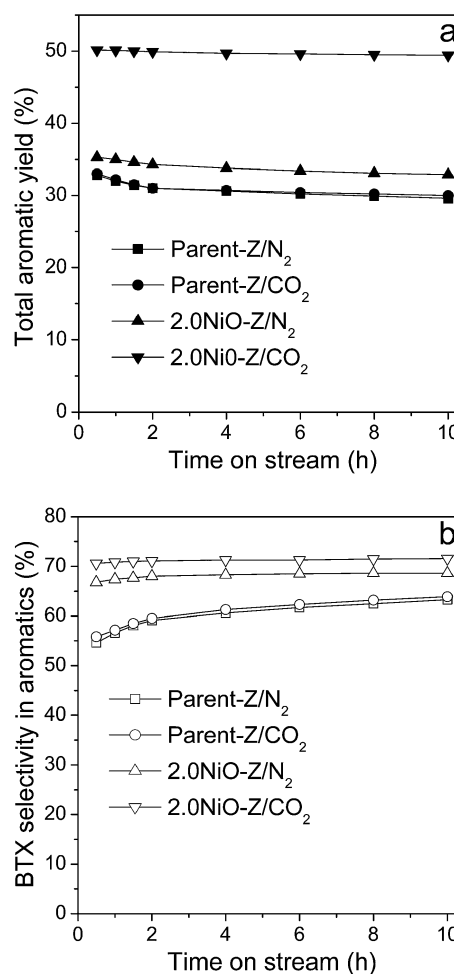


Fig. 6 The time on-stream total aromatics yield (a) and BTX selectivity (in aromatics) (b) in the MTA reaction over parent-Z and 2.0NiO-Z under N₂ and CO₂ atmospheres.

an evident decline of activity of parent-Z and 2.0NiO-Z under N₂ atmosphere was observed, with an obvious increase of BTX selectivity. However, 2.0NiO-Z showed the highest catalytic stability under CO₂ atmosphere; there was hardly any decline for total aromatic yield in 10 h reaction. To understand the difference in catalytic stability, the coke on the used catalysts was analysed by TG, and the framework and porous structure of the used catalysts were studied by BET and XRD after removing coke by calcination. Then, the valence-state of Ni species on the used 2.0NiO-Z in N₂ and CO₂ atmospheres was also determined by H₂-TPR.

In the MTA reaction, 1,3,5-trimethylbenzene is the smallest-sized coke molecule in the HZSM-5 channel, and its boiling point is 438 K. Therefore, it can be confirmed that the loss of coke begins at 438 K in TG analysis.³⁹ As can be seen in Fig. 7, the mass loss at the temperature range of 438–773 K was ascribed to soluble coke (large organic molecules), while that at 773–1023 K corresponded to the insoluble coke (with high mole ratio of C/H) formed from soluble coke.^{53,39} The coke amounts on the used parent-Z in N₂ and CO₂ atmospheres were up to 5.63% and 5.70% respectively. Moreover, the results of XRD (shown in Fig. 8) and BET (listed in Table 6) for the used catalysts after removing coke prove that the framework and porous structure of these catalysts were not destroyed during the 10 h reaction. These facts indicate that serious coke deposition resulted in the obvious decline of parent-Z activity, owing to the high density of strong acid sites, which is in favor of deep reaction of aromatics and coke formation.^{27,51,54,55} With coke covering more and more strong acid sites, the rates of coke deposition and activity decline decreased gradually (as can be seen in Fig. 6).

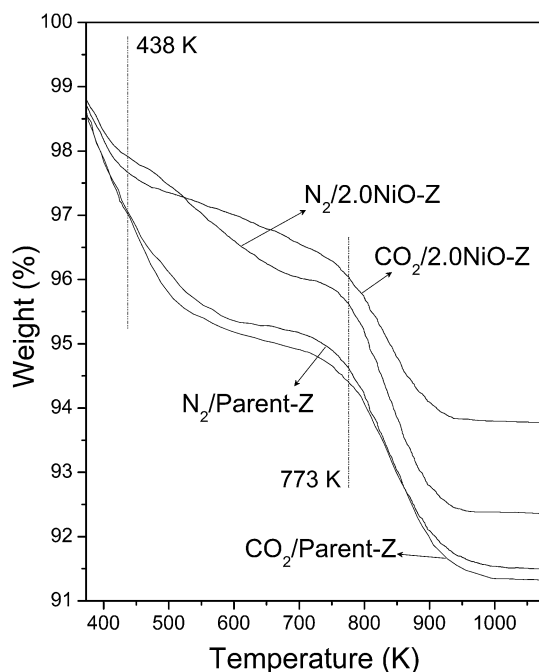


Fig. 7 TG curves of the used parent-Z and 2.0NiO-Z in aromatization for 10 h under N₂ and CO₂ atmospheres.

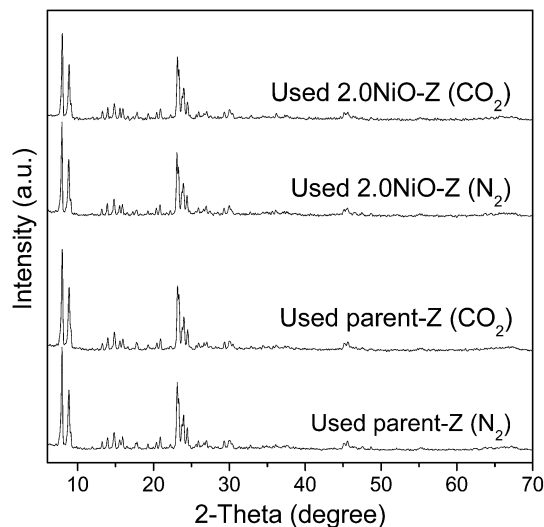


Fig. 8 XRD patterns of the used parent-Z and 2.0NiO-Z after removing coke.

Table 6 Specific surface areas and pore volumes of the used parent-Z and 2.0NiO-Z after removing coke

| Catalyst | Surface area (m ² g ⁻¹) | | | Pore volume (ml g ⁻¹) | |
|---------------------------|--|----------|----------|-----------------------------------|-----------|
| | Total (BET) | External | Internal | Mesopore | Micropore |
| N ₂ -parent-Z | 336.1 | 58.1 | 278.0 | 0.060 | 0.118 |
| CO ₂ -parent-Z | 336.7 | 58.3 | 278.4 | 0.061 | 0.119 |
| N ₂ -2.0NiO-Z | 324.3 | 51.7 | 272.6 | 0.056 | 0.114 |
| CO ₂ -2.0NiO-Z | 324.9 | 51.9 | 273.0 | 0.056 | 0.115 |

Although the coke on the used 2.0NiO-Z in N₂ atmosphere was less than that on the used parent-Z owing to the relative weak acidity (of 2.0NiO-Z), which can prevent the strong deep reaction of aromatics and to a certain extent reduce coke formation,^{27,51,54} it is still up to 5.33%. Nevertheless, that on the used 2.0NiO-Z in CO₂ atmosphere was much less (only 3.85%). Besides, as shown in Table 7, about 48.5% NiO on 2.0NiO-Z was reduced to Ni in the 10 h reaction under N₂ atmosphere, while 87.7% NiO was retained in CO₂ atmosphere. The above facts imply that CO₂ activated by NiO species not only can restrict the carbonaceous deposition by reaction with partial adjacent coke,^{28,30} but also can effectively suppress the reduction of highly active NiO species in the reaction.^{28,30} These effects of activated CO₂ and the appropriate

Table 7 The H₂ consumption in H₂-TPR and the Ni/NiO molar ratio for the fresh 2.0NiO-Z and used 2.0NiO-Z in the MTA reactions for 10 h

| Catalyst | H ₂ consumption (mmol g ⁻¹) | Ni/NiO molar ratio |
|------------------------------------|--|--------------------|
| Fresh | 0.33 | 0 |
| Used in CO ₂ atmosphere | 0.29 | 0.14 |
| Used in N ₂ atmosphere | 0.17 | 0.94 |

acidity of 2.0NiO-Z ensure the high catalytic stability of this catalyst in CO₂ atmosphere.

4. Conclusions

Conversion of methanol to aromatics was investigated over parent HZSM-5 and NiO-HZSM-5 in a fixed-bed reactor under CO₂ and N₂ flow. CO₂ atmosphere significantly improved the aromatization activity and BTX yield over NiO-HZSM-5. Hydrocarbon dehydrogenation was coupled with the reverse water-gas shift reaction by CO₂ activated over NiO species. The coupled reaction not only can effectively promote dehydrogenation of alkanes to form olefin intermediates, but also can accelerate dehydrogenation in the conversion of olefin intermediates to aromatics, promoting methanol aromatization under the cooperation between the acid sites and the activated CO₂ on the NiO-HZSM-5 catalyst. An optimized NiO-HZSM-5 with 2.0 wt% NiO loading exhibited 50.1% total aromatic yield and 35.5% BTX yield under CO₂ atmosphere. It also showed high catalytic stability resulting from the restriction of its acidity on coking, carbonaceous elimination by the activated CO₂-reacting deposited coke, and the suppression of activated CO₂ on the reduction of highly active NiO species.

Acknowledgements

This work was financially supported by Shanghai Key Basic Research (Grant no. 11JC1412500) and National Natural Science Foundation of China (Grant no. 51174277).

References

- M. Weckhuysen, D. J. Wang, M. P. Rosynek and J. H. Lunsford, *J. Catal.*, 1998, **175**, 338–346.
- Y. B. Song, C. Y. Sun, W. J. Shen and L. W. Lin, *Appl. Catal., A*, 2007, **317**, 266–274.
- D. M. Ren, X. S. Wang, G. Li and H. O. Liu, *Chin. J. Catal.*, 2010, **31**, 348–352.
- J. H. Yang, S. X. Yu, H. Y. Hu, N. B. Chu, J. M. Lu, D. H. Yin and J. Q. Wang, *Chin. J. Catal.*, 2011, **32**, 362–367.
- S. Q. Ma, X. G. Guo, L. X. Zhao, S. Scott and X. H. Bao, *J. Energy Chem.*, 2013, **22**, 1–20.
- Z. H. Jin, S. Liu, L. Qin, Z. C. Liu, Y. D. Wang, Z. K. Xie and X. Y. Wang, *Appl. Catal., A*, 2013, **453**, 295–301.
- X. Y. Yin, N. B. Chu, J. H. Yang, J. Q. Wang and Z. F. Li, *Catal. Commun.*, 2014, **43**, 218–222.
- J. F. Haw, W. G. Song, D. M. Marcus and J. B. Nicholas, *Acc. Chem. Res.*, 2003, **36**, 317–326.
- J. G. Zhang, W. Z. Qian, X. P. Tang, K. Shen, T. Wang, X. F. Huang and F. Wei, *Acta Phys.-Chim. Sin.*, 2013, **29**, 1281–1288.
- Q. Y. Wang, S. T. Xu, J. R. Chen, Y. X. Wei, J. Z. Li, D. Fan, Z. X. Yu, Y. Qi, Y. L. He, S. L. Xu, C. Y. Yuan, Y. Zhou, J. B. Wang, M. Z. Zhang, B. L. Su and Z. M. Liu, *RSC Adv.*, 2014, **4**, 21479–21491.
- W. Fang, J. Tang, X. C. Huang, W. B. Shen, Y. B. Song and C. Y. Sun, *Chin. J. Catal.*, 2010, **31**, 264–266.
- T. Tian, W. Z. Qian, X. P. Tang, S. Yu and F. Wei, *Acta Phys.-Chim. Sin.*, 2010, **26**, 3305–3309.
- Y. M. Ni, A. M. Sun, X. L. Wu, G. L. Hai, J. L. Hu, T. Li and G. X. Li, *Microporous Mesoporous Mater.*, 2011, **143**, 435–442.
- M. Conte, J. A. Lopez-Sanchez, Q. He, D. J. Morgan, Y. Ryabenkova, J. K. Bartley, A. F. Carley, S. H. Taylor, C. J. Kiely, K. Khalid and G. J. Hutchings, *Catal. Sci. Technol.*, 2012, **2**, 105–112.
- J. A. Lopez-Sanchez, M. Conte, P. Landon, W. Zhou, J. K. Bartley, S. H. Taylor, A. F. Carley, C. J. Kiely, K. Khalid and G. J. Hutchings, *Catal. Lett.*, 2012, **142**, 1049–1056.
- Q. Miao, M. Dong, X. J. Niu, H. Wang, W. B. Fan, J. G. Wang and Z. F. Qin, *J. Fuel Chem. Technol.*, 2012, **40**, 1230–1239.
- W. Q. Liu, W. N. Lei, T. M. Shang, W. H. Li, Q. F. Zhou, H. Q. Wang and J. Ren, *Chem. Ind. Eng. Prog.*, 2011, **30**, 1967–1976.
- H. A. Zaidi and K. K. Pant, *Catal. Today*, 2004, **96**, 155–160.
- Y. H. Zhao and C. Y. Cao, *Petrochem. Technol.*, 2011, **40**, 831–834.
- R. Barthos, T. Bansagi, T. S. Zakar and F. Solymosi, *J. Catal.*, 2007, **247**, 368–378.
- X. J. Jiao, C. Yang, Z. X. Di, X. J. Guo and J. H. Wu, *Adv. Mater. Res.*, 2011, **233–235**, 202–205.
- Y. M. Ni, A. M. Sun, X. L. Wu, J. L. Hu, T. Li and G. X. Li, *Chin. J. Chem. Eng.*, 2011, **19**, 439–445.
- U. V. Mentzel, K. T. Højholt, M. S. Holm and R. Fehrmann, *Appl. Catal., A*, 2012, **417–418**, 290–297.
- Y. B. Xin, P. Y. Qi, X. P. Duan, H. Q. Lin and Y. Z. Yuan, *Catal. Lett.*, 2013, **143**, 798–806.
- C. Song, K. F. Liu, D. Z. Zhang, S. L. Liu, X. J. Li, S. J. Xie and L. Y. Xu, *Appl. Catal., A*, 2014, **470**, 15–23.
- A. Q. Zheng, Z. L. Zhao, S. Chang, Z. Huang, Z. Zhao, H. X. Wu, X. B. Wang, F. He and H. B. Li, *Green Chem.*, 2014, **16**, 2580–2586.
- J. H. Li, Y. N. Wang, W. Z. Jia, Z. W. Xi, H. H. Chen, Z. R. Zhu and Z. H. Hu, *J. Energy Chem.*, in press.
- J. F. Ding, Z. F. Qin, S. W. Chen, X. K. Li, G. F. Wang and J. G. Wang, *J. Fuel Chem. Technol.*, 2010, **38**, 458–461.
- X. L. Zhang, M. Yan, H. W. Lv and S. Gao, *Nat. Gas Chem. Ind.*, 2009, **34**(4), 35–38.
- J. F. Ding, Z. F. Qin, X. K. Li, G. F. Wang and J. G. Wang, *J. Mol. Catal. A: Chem.*, 2010, **315**, 221–225.
- C. H. Yoon and G. J. Kim, *Kongop Hwahak*, 1997, **8**, 543–549.
- F. Z. Zhang and B. Q. Xu, *Prog. Chem.*, 2002, **14**, 56–60.
- J. W. Wang and S. H. Gu, *Prog. Chem.*, 1998, **10**, 374–380.
- J. Scherzer, *J. Catal.*, 1978, **54**, 285–288.
- F. Pompeo, N. N. Nichio, M. G. Gonzalez and M. Montes, *Catal. Today*, 2005, **107–108**, 856–862.
- A. H. Fakeeha, W. U. Khan, A. S. Al-Fatesh and A. E. Abasaheed, *Chin. J. Catal.*, 2013, **34**, 764–768.
- A. J. Maia, B. Louis, Y. L. Lam and M. M. Pereira, *J. Catal.*, 2010, **269**, 103–109.
- J. Gao, Z. Y. Hou, J. Z. Guo, Y. H. Zhu and X. M. Zheng, *Catal. Today*, 2008, **131**, 278–284.
- J. H. Li, H. Xiang, M. Liu, Q. L. Wang, Z. R. Zhu and Z. H. Hu, *Catal. Sci. Technol.*, 2014, **4**, 2639–2649.

- 40 W. Zou, D. Q. Yang, Z. R. Zhu, D. J. Kong, Q. L. Chen and Z. Gao, *Chin. J. Catal.*, 2005, **26**, 470–474.
- 41 Z. R. Zhu, Q. L. Chen, W. Zhu, D. J. Kong and C. Li, *Catal. Today*, 2004, **93–95**, 321–332.
- 42 Z. R. Zhu, Q. L. Chen, Z. K. Xie, W. M. Yang, D. J. Kong and C. Li, *J. Mol. Catal. A: Chem.*, 2006, **248**, 152–158.
- 43 L. J. Jin, Y. M. Fang and H. Q. Hu, *Catal. Commun.*, 2006, **7**, 255–259.
- 44 J. N. Parka, J. Wangb, S. I. Hongc and C. W. Lee, *Appl. Catal., A*, 2005, **292**, 68–75.
- 45 L. J. Jin, H. Q. Hu, X. Y. Wang and C. Liu, *Ind. Eng. Chem. Res.*, 2006, **45**, 3531–3536.
- 46 G. S. Sun, Q. Z. Huang, H. Q. Li, H. T. Liu, Z. Zhang, X. R. Wang, Q. P. Wang and J. S. Wang, *Chin. J. Catal.*, 2011, **32**, 1424–1429.
- 47 F. Zhang, Ph.D. thesis, Fudan University, 2012.
- 48 F. Xie, H. S. Li, X. L. Zhao, F. Ren, D. Z. Wang, J. F. Wang and J. L. Liu, *Chin. J. Catal.*, 2004, **25**, 403–408.
- 49 G. X. Dong and L. Zhang, *Chin. J. Catal.*, 1995, **16**, 183–189.
- 50 J. W. Wang, Z. X. Zhang and X. K. Wang, *J. Mol. Catal.*, 2000, **14**, 15–19.
- 51 K. Y. Lee, M. Y. Kang and S. K. Ihm, *J. Phys. Chem. Solids*, 2012, **73**, 1542–1545.
- 52 Q. Jin, Z. L. Cheng, H. Y. Li, J. Z. Gui, N. N. Liu, X. T. Zhang, K. X. Qi and Z. L. Sun, *J. Petrochem. Univ.*, 1999, **12**, 5–10.
- 53 J. Li, G. Xiong, Z. Feng, Z. Liu, Q. Xin and C. Li, *Microporous Mesoporous Mater.*, 2000, **39**, 275–280.
- 54 M. Guisnet, L. Costa and F. R. Ribeiro, *J. Mol. Catal. A: Chem.*, 2009, **305**, 69–83.
- 55 U. Olsbye, S. Svelle, M. Bjørgen, P. Beato, T. V. W. Janssens, F. Joensen, S. Bordiga and K. P. Lillerud, *Angew. Chem., Int. Ed.*, 2012, **51**, 5810–5831.